Transcriptome and metabolome response of eggplant against Ralstonia solanacearum infection

Xi Ou Xiao [Corresp., 1, 2, 3], **Wenqiu Lin** [1, 2, 3], **Enyou Feng** [4], **Xiongchang Ou** [1, 2, 3]

[1] South Subtropical Crop Research Institute Chinese Academy of Tropical Agricultural Sciences (CATAS), Zhanjiang, Guangdong, □□

[2] Key Laboratory for Post-harvest Physiology and Technology of Tropical Horticultural Products of Hainan Province, Zhanjiang, Guagndong, □□

[3] Zhanjiang City Key Laboratory for Tropical Crops Genetic Improvement, Zhanjiang, Guangdong, □□

[4] Zhanjiang Academy of Agricultural Sciences, Zhanjiang, Guangdong, □□

Corresponding Author: Xi Ou Xiao
Email address: xiao-forlearning@catas.cn

Bacterial wilt is a soil-borne disease that represents ubiquitous threat to *Solanaceae* crops. The whole-root transcriptomes and metabolomes of bacterial wilt-resistant eggplant were studied to understand the response of eggplant to bacterial wilt. A total of 2896 differentially expressed genes and 56 differences in metabolite were identified after inoculation with *Ralstonia solanacearum*. Further analysis showed that the biosynthesis pathways for phytohormones, phenylpropanoid, and flavonoids were altered in eggplant after inoculation with *R. solanacearum*. The results of metabolomes also showed that phytohormones played a key role in eggplant resistance to bacterial wilt. The integrated analyses of the transcriptomic and metabolic datasets indicated that jasmonic acid (JA) and the JA signaling pathway positively regulated eggplant resistance to bacterial wilt. These findings remarkably improve our understanding of the mechanisms of induced defense response in eggplant and will provide new clues for the development of disease-resistant varieties of eggplant.

Transcriptome and metabolome response of eggplant against *Ralstonia solanacearum* infection

Xi'ou Xiao[1,2,4*], Wenqiu Lin [1,2,4], Enyou Feng[3], Xiongchang Ou [1,2,4]

[1]South Subtropical Crop Research Institute Chinese Academy of Tropical Agricultural Sciences (CATAS), Zhanjiang City ,Guangdong Province, China

[2] Key Laboratory for Post-harvest Physiology and Technology of Tropical Horticultural Products of Hainan Province,Zhanjiang City, Guangdong Province, China

[3] Zhanjiang Academy of Agricultural Sciences, Zhanjiang City, Guangdong Province, China

[4]Zhanjiang City Key Laboratory for Tropical Crops Genetic Improvement, Zhanjiang City, Guangdong Province, China

***Corresponding Author:**

Xi'ou Xiao

She tuan road, Zhanjiang City, Guangdong Province, 524091 , China

Xiao-forlearning@163.com

Abstract: Bacterial wilt is a soil-borne disease that represents ubiquitous threat to *Solanaceae* crops. The whole-root transcriptomes and metabolomes of bacterial wilt-resistant eggplant were studied to understand the response of eggplant to bacterial wilt. A total of 2896 differentially expressed genes and 56 differences in metabolite were identified after inoculation with *Ralstonia solanacearum*. Further analysis showed that the biosynthesis pathways for phytohormones, phenylpropanoid, and flavonoids were altered in eggplant after inoculation with *R. solanacearum*. The results of metabolomes also showed that phytohormones played a key role in eggplant resistance to bacterial wilt. The integrated analyses of the transcriptomic and metabolic datasets indicated that jasmonic acid (JA) and the JA signaling pathway positively regulated eggplant resistance to bacterial wilt. These findings remarkably improve our understanding of the mechanisms of induced defense response in eggplant and will provide new clues for the development of disease-resistant varieties of eggplant.

Keywords: Bacterial wilt, Eggplant, JA signaling pathway, Metabolomes, Transcriptomes

INTRODUCTION

Eggplant (*Solanum melongena* L.) is an important vegetable in tropical and subtropical areas. According to FAO, 55,197,878 tons of eggplant fruit were produced worldwide in 2019. The eggplant fruit contains a variety of nutrients, such as vitamins, phenolics, and antioxidants that

are beneficial to human health (Gurbuz et al., 2018). At the same time, diseases, such as bacterial (Barik et al., 2020) and verticillium wilts (Yang et al., 2019), can lead to significant yield loss.

Bacterial wilt is a soil-borne disease caused by the pathogen *Ralstonia solanacearum*. The pathogen has more than 450 host plant species, which belong to 54 families (Jiang et al., 2017). Bacterial wilt is one of the most destructive plant diseases because it is difficult to control and can cause considerable production losses. No effective chemical management strategy for bacterial wilt disease is available to date. In field practice, the management and control of bacterial wilt includes resistant cultivar selection (Barik et al., 2020), grafting (Manickam et al., 2021), crop rotation (Ayana and Fininsa, 2017), and antagonistic organism (Yuliar et al., 2015). Among these management practices, the resistant cultivar selection is the most economical and efficient means.

Many QTLs（quantitative trait locus） resistant to bacterial wilt are identified in different plants, such as eggplant (Salgon et al., 2017，2018), tomato(Kim et al., 2018;Abebe et al., 2020) , potato(Habe et al., 2019), and peanut (Wang et al., 2018;Luo et al., 2019). These QTLs provide a good foundation for molecular marker-assisted selection and gene editing for breeding resistant cultivars. However, the mechanisms of plants regulating defense response remain limited. How the plant responds to bacterial wilt should be understood to breed resistant varieties efficiently and improve coping ability.

Once a plant detects pathogen invasion, the plant initiates a defense response against the disease, including the expression of defense gene and biosynthesis of secondary metabolites. Secondary metabolites, such as alkaloids, flavonoids, and phenolics, have been reported to play a key role in plant defense reaction (Zaynab et al., 2018). Also, phytohormones, such as salicylic acid (SA), jasmonic acid (JA), and ethylene (ET), and their signaling pathways play a key role in plant disease defense response(Dong, 1998). Individual hormones and their crosstalk play an essential role in fine tuning defense responses to phytopathogen(Feys and Parker, 2000). .

Genome-wide transcriptome profiling has been conducted in plant response to *R. solanacearum* interaction. Results showed that a set of genes is remarkable differentially expressed after the plant is attacked by *R. solanacearum*. For example, 9831 DEGs, including WRKY transcription factors, ERFs transcription factors, and defense-related genes, in tobacco respond to *R. solanacearum* infection. The Kyoto Encyclopedia of Genes and Genomes (KEGG) analysis demonstrated phenylpropane pathways as primary resistance pathways to *R.*

solanacearum infection(Li et al., 2021c). In the *Arabidopsis* root, 2698 DEGs are identified after *R. solanacearum* infection. The DEGs involved in multiple-hormone signaling cascades include abscisic acid (ABA), auxin, JA, and ET. In *Casuarina equisetifolia–R.solanacearum* interaction, 479 DEGs, which are classified into brassinosteroid, SA, and JA signaling pathways, are detected (Wei et al., 2021).

Except transcriptomics, other omics, such proteomics and metabolomics, have been widely used to analyze plant biotic and abiotic stress responses. Metabolomics is focused on all small molecular components and widely used to study plant biological function and mechanism. Metabolomics is attaining increasing attention in pathogen–plant interaction to elucidate plant defense mechanisms (Shulaev et al., 2008; Chen et al., 2019). Multiomics data especially combined metabolomic and transcriptomic analysis is integrated and analyzed to understand the complex signaling pathways in plant defense reaction (Yuan et al., 2018;Su et al., 2020;Wei et al., 2021).

In this study, we perform comparative transcriptomic and metabolomic analyses after *R. solanacearum* inoculation into bacterial wilt-resistant eggplant to understand the defense responses of eggplant against bacterial wilt. *R. solanacearum*-induced DEGs and metabolites are identified. Results extend our understanding of the molecular mechanism of eggplant response to *R. solanacearum*.

MATERIAL AND METHODS

Plant material

Eggplant inbred line “NY-1” (R genotype, highly resistant to bacterial wilt) was obtained from the South Subtropical Crop Research Institute Chinese Academy of Tropical Agricultural Sciences. Seeds were sown in 15 cm diameter pots. The growing material was placed in pots and composed of sterile vermiculite and clay mixed in a 3:1 volume/volume ratio. Seedlings were grown under 28 °C /25 °C day/night temperatures with a 16 h light/8 h dark photoperiod condition. After four weeks of culture, when seedlings were at the 4-leaf stage, the culture was incubated with *R. solanacearum*.

Bacterial strain and inoculation

The *R. solanacearum* strain GMI1000-tac-EGFP was grown overnight on 2,3,5-triphenyl tetrazolium chloride medium at 28 °C and suspended in sterile distilled water(Xi-ou et al., 2021).

The suspension was adjusted to 0.12 (108 colony-forming units/ml) at 600 nm. The roots of eggplants were cut at 0–1 cm from the apex and then inoculated in 50 ml suspended *R. solanacearum*. After inoculation with *R. solanacearum*, plants were grown under 30 °C/32 °C day/night temperatures with a 16 h light/8 h dark photoperiod condition. Disease was rated on a scale of 0 to 4: 0 = no symptoms, 1 = 0%–25% leaves wilted, 2 = 25%–50% leaves wilted, 3 = 50%–75% leaves wilted, 4 = 75%–100% wilted and plant dead. DI (%) was calculated using the formula: DI = ((N0 × 0 + N1 × 1 + N2 × 2 + N3 × 3 + N4 × 4) / (total number of plants)). N0 to N4 were the number of plants with disease rating scale values of 0 to 4, respectively. The EGFP fluorescence of *R. solanacearum* was detected by the LuYour3415.

RNA-seq

The statistical power of this experimental design, calculated in RNASeqPowe is 0.9. Values for alpha and CV were 0.05. The effect parameter was 2. The sample size results at 6x sequencing depths were 7.55. At 0, 24, and 48 hpi, the roots of 10 eggplants were collected, mixed, immediately frozen in liquid nitrogen, and stored at −80 °C. All three biological replicates were established in each treatment. Total RNAs were extracted using the Spin Column Plant total RNA Purification Kit (Sangon Biotech, Shanghai, China) following the manufacturers' protocol. RNA quantification was performed using the Qubit RNA Assay Kit in Qubit 2.0 Fluorometer. RNA integrity was assessed by the RNA Nano 6000 Assay Kit of the Agilent Bioanalyzer 2100 system. After the Illumina sequencing libraries were established, cDNA libraries were sequenced on the Illumina HiSeq platform. mRNA-Seq was assembled and analyzed by the Guangzhou Gene Denovo Biotechnology Corporation (Guangzhou, China).

After trimming adapter sequences and removing low-quality reads by using the FastQC tool with default parameters, reads were aligned to the eggplant reference genome(Barchi et al., 2019) using HISAT2(version 2.1.0). The differential expression analysis of two groups was performed using the DESeq2 R package (version 1.10.1)(Love et al., 2014). For identifying DEGs, absolute fold change ≥ 2 and false discovery rate (FDR) < 0.01 were used as screening criteria. The expression patterns of DEGs were analyzed using the Mfuzz R package (Kumar et al., 2007).

Metabolite profiling using UPLC-MS/MS

The freeze-dried eggplant root was crushed using a mixer mill (MM 400, Retsch) with a zirconia bead for 1.5 min at 30 Hz. About 100 mg lyophilized powder was dissolved with 1.2 ml of 70% methanol solution. The solution was vortexed six times for 30 s every 30 min, placed in a refrigerator at 4 °C overnight, and centrifuged at 12,000rpm for 10 min. Extracts were filtered (SCAA-104, 0.22 μm pore size) before UPLC-MS/MS analysis.

UPLC conditions

Sample extracts were analyzed using an UPLC-ESI-MS/MS system (UPLC, SHIMADZU Nexera X2, www.shimadzu.com.cn/; MS, Applied Biosystems 4500 Q TRAP, www.appliedbiosystems.com.cn/). Analytical conditions were as follows. The UPLC column was Agilent SB-C18 (1.8 μm, 2.1 mm × 100 mm). The mobile phase consisted of solvents A (pure water with 0.1% formic acid) and B (acetonitrile with 0.1% formic acid). Sample analyses were performed with a gradient program that employed the starting conditions of 95%A and 5% B. Within 9 min, a linear gradient to 5% A and 95% B was programmed and kept for 1 min. Subsequently, a composition of 95% A and 5.0 % B was adjusted within 1.10 min and kept for 2.9 min. The flow velocity was set as 0.35 ml/min. The column oven was set to 40 °C. The injection volume was 4 μl. The effluent was alternatively connected to an ESI-triple quadrupole-linear ion trap (QTRAP)-MS.

ESI-Q TRAP-MS/MS

LIT and triple quadrupole (QQQ) scans were acquired on the QTRAP-MS and AB4500 Q TRAP UPLC/MS/MS System equipped with an ESI Turbo Ion-Spray interface operating in positive and negative ion modes and controlled by the Analyst 1.6.3 software (AB Sciex). ESI source operation parameters were as follows: ion source, turbo spray; source temperature 550 °C; ion spray voltage (IS), 5500 V (positive ion mode)/−4500 V (negative ion mode); ion source gas I, gas II, and curtain gas set to 50, 60, and 25.0 psi, respectively; and high collision-activated dissociation. Instrument tuning and mass calibration were performed with 10 and 100 μmol/l polypropylene glycol solutions in QQQ and LIT modes, respectively. QQQ scans were acquired through MRM experiments with collision gas (nitrogen) set to medium. DP and CE for individual MRM transitions were done with further DP and CE optimization. A specific set of MRM transitions was monitored for each period in accordance with the metabolites eluted within this period.

Data analysis

Quality control (QC) samples were prepared by mixing sample extracts. A QC sample was inserted into each of the 10 detected samples during the stability evaluation of analytical conditions. The metabolome was identified in accordance with the metware database and quantified by multiple reaction monitoring.

Significantly regulated metabolites between groups were determined by VIP $\geq$ 1 and absolute Log2FC $\geq$ 1. VIP values were extracted from OPLS-DA results, which also contained score and permutation plots generated using the R package MetaboAnalystR. Data were subjected to log transformation (log2) and mean centering before OPLS-DA. A permutation test (200 permutations) was performed to avoid overfitting.

KEGG annotation and enrichment analyses

Identified metabolites were annotated using the KEGG Compound database (http://www.kegg.jp/kegg/compound/), and annotated metabolites were then mapped to the KEGG Pathway database. Pathways with significantly regulated metabolites were then fed into metabolite set enrichment analysis, and their significance was determined by hypergeometric test's p-values.

RESULTS

Analysis of the bacterial wilt resistance of eggplant

After the R and S genotypes of eggplant material were inoculated with the GMI1000-tac-EGFP strain, the disease index (DI) and EGFP fluorescence were analyzed. Results showed that 10 days after inoculation with R. solanacearum, the DIs of R and S were 0 and 2.48, respectively (Figure 1A). R genotypes showed normal results, whereas S genotypes showed wilt (Figure 1B). EGFP fluorescence was detected at S stem and root but was not observed at the R stem and root (Figures 1C and 1D). This result showed that R genotypes were highly resistant to GMI1000.

Induced responses to bacterial wilt in global transcriptome changes of eggplant

The sample size is 7.40

The transcriptome was compared after inoculation of the GMI1000-tac-EGFP to understand the mechanism of bacterial wilt defense response of eggplant. Three time points (i.e., 0, 24, and 48 h postinoculation [hpi]) were analyzed.

Approximately 390.98 million clean reads were generated for nine samples (Table 1). About 85% clean reads were aligned to the eggplant reference genome. Transcriptomic sequences were deposited in the NCBI Sequence Read Archive under accession number PRJNA837016.

PCA showed that the first two PCAs explained 59.48% of the total variation (Figure 2A). The heatmap of DEGs showed a significant difference in gene expression level after the inoculation of *R. solanacearum* (Figure 2B). After filtration by FDR < 0.01 and absolute Log2(fold change [FC]) ≥ 1, 1831 (799 upregulated and 1032 downregulated), 1416 (708 upregulated and 708 downregulated), and 1032 (538 upregulated and 494 downregulated) DEGs were identified in R-0h_vs_R-24h, R-0h_vs_R-48h, and R-24h_vs_R-48h, respectively (Figure 2C). These DEGs are listed in Tables S1–S3.

A total of 485 and 751 genes were upregulated and downregulated, respectively, in at least one time point. At R-24h and R-48h, 339 and 328 genes were upregulated and downregulated, respectively. Four genes were common in the R-0h_vs_R-24hUp and R-0h_vs_R-48hDn sets, and a gene was common in the R-0h_vs_R-24hDn and R-0h_vs_R-48hUp sets (Figure 3).

KEGG and KOG classification of DEGs

DEGs were mapped to the KEGG pathway to understand DEG function in the eggplant defense response. The top 20 pathways included metabolic pathways, biosynthesis of secondary metabolites, plant hormone signal transduction, MAPK signaling pathway, plant–pathogen interaction, and flavonoid biosynthesis pathway (Figure S1). KOG classification results showed signal transduction mechanisms and defense mechanism classification (Figure S2).

Expression pattern analysis of DEGs

A set of genes with similar expression patterns was functionally correlated. Twelve expression patterns were obtained in accordance with RNA-seq data. A total of 537 (subclasses 3 and 9) and 526 (subclasses 2 and 7) DEGs were maintained to be upregulated and downregulated at 24 and 48 h (Figure 4).

Widely targeted metabolome analysis

On the basis of UPLC-MS/MS and Metware metabolite database, 661 metabolomics were detected (Table S4). PCA results showed that the first two components could explain 42.23% of dataset variation (Figure 5A). Cross-validation indicated the first two components relevant for the classification of variation, which illustrated different directions of response to *R.*

solanacearum. The heatmap showed different expression profiles after inoculation with *R. solanacearum* (Figure 5B). A total of 44 (11 upregulated and 33 upregulated), 25 (6 upregulated and 19 upregulated), and 24 (14 upregulated and 10 upregulated) differential metabolites were identified in R-0h_vs_R-24h, R-0h_vs_R-48h, and R-24h_vs_R-48h, respectively (Figure 5C). Differential metabolites are listed in Tables S5–S7.

A total of 15 and 41 metabolites were upregulated and downregulated, respectively, in at least one time point. A total of 2 and 11 metabolites were upregulated and downregulated, respectively, at R-24h and R-48h (Figure 6).

KEGG of differential metabolites

KEGG classification results showed that the top pathways were metabolic pathways and biosynthesis of secondary metabolites (Figure S3). Several genes were involved in phenylpropanoid biosynthesis, flavone and flavonol biosynthesis, and plant hormone signal transduction pathway.

Expression pattern analysis of metabolites

A set of metabolites with similar expression patterns was functionally correlated. Twelve expression patterns were obtained in accordance with metabolome data (Figure 7). A total of 101 (subclasses 1 and 6) and 132 (subclasses 4 and 5) metabolites were kept upregulated and downregulated at R-24h and R-48h (Figure 7).

Integration analysis of transcriptomic and metabolic datasets

DEGs and differential metabolites were simultaneously assigned to KEGG pathways ($p < 0.05$) to understand the resistance mechanism of eggplant resistance to bacterial wilt. Results showed that only alpha-Linolenic acid metabolism (ko00592) and plant hormone signal transduction pathway (ko04075) were significantly enriched in the R-0h vs. R-24h group (Figure S4). The metabolites involved in these two pathways were JA, ABA, jasmonate, and 9-Hydroxy-12-oxo- 15(Z)-octadecenoic acid. However, 69 genes were involved in these two pathways (Table S8). The ko00592 pathway finally biosynthesis the Methyl-jasmonate which was the precursor of JA biosynthesis (Figure S5).

Transcriptome and metabolome data were also compared by the Pearson correlation analysis (Pearson correlation coefficient > 0.8). Gene–metabolite correlation networks were also constructed (Figure 8). In the R-0h vs. R24 group, SMEL_008g298210.1，

SMEL_011g363600.1, and SMEL_005g223990.1 were highly correlated with JA. SMEL_003g183930.1 and SMEL_006g251030.1 were highly correlated with ABA. In the R-0h vs. R-48h group, 13 genes were highly correlated with (−)-Jasmonoyl-L-Isoleucine. These results showed that JA might regulate the gene expression in the bacterial wilt resistance defense of eggplant.

DISCUSSION

Breeding resistant crops is the most efficient process in the control of bacterial wilt. Besides the marker-assisted selection, gene modification and novel genetic editing technologies by CRISP/Cas9 are efficient approaches to develop resistant cultivars. Understanding the resistance mechanism and cloning the defense-related gene will accelerate the use of these strategies to develop resistant crops. To the best of our knowledge, the present study is the first effort to integrate transcriptomic and metabolic techniques and analyze the defense responses of eggplant to bacterial wilt. Results enhance our understanding of the mechanisms underlying the responses of eggplant to bacterial wilt.

The plant defense reaction is a complicated development course of physiological and biochemical changes. The plant hormone signal transduction, MAPK signaling pathway, plant–pathogen interaction pathway, and flavonoid biosynthesis pathway are involved in bacterial wilt disease response (Ishihara et al., 2012; Jiang et al., 2019; Chen et al., 2018; Dai et al., 2019; Li et al., 2021a; Li et al., 2021c; Wei et al., 2021). Flavonoids are reported to play a key role in plant resistance (Treutter, 2006). After *R. solanacearum* attack, flavonoids are of prime importance in tomato and *Casuarina equisetifolia* defense responses (Zeiss et al., 2018;2019;Wei et al., 2021). In the present study, the KEGG enrichment analysis of DEGs and differential metabolites shows that flavonoids play an important role in eggplant response to *R. solanacearum*.

Phytohormones, such as SA and JA, play a key role in plant response to biotic stress(Dong, 1998;Feys and Parker, 2000). Several results showed that SA plays an important role in bacterial wilt defense (Na et al., 2016;Chen et al., 2018;Zeiss et al., 2018). In the present study, the SA content and genes involved in the SA signaling pathway, such as NPR1 and PR1, are different after the eggplant inoculation with *R. solanacearum*. However, our results indicated that JA also plays a key role in eggplant response to *R. solanacearum*. The contents of JA and JA synthesis precursor, such as (−)-Jasmonoyl-L-Isoleucine, increase after inoculation with *R. solanacearum*.

The JA signaling-related gene, such as JAZ and MYC2, is upregulated. Chen et al. (2018) also showed that the expression levels of JAZ and MYC2 are upregulated after inoculation of eggplant with *R. solanacearum*. JAZ and MYC2 are master regulators in the JA signaling pathway. JAZ and MYC2 regulate the JA-mediated plant immunity. The overexpression of OsMYC2 increases the early JA-responsive gene expression and the bacterial blight resistance in rice (Yuya et al., 2016).

Also, the integrated transcriptomic and metabolic analysis showed that JA positively regulates bacterial wilt resistance. On the basis of the literature and our results, we speculated the JA biosynthesis and signaling cascade in eggplant response to *R. solanacearum* (Figure 9). Although several results showed that *Pseudomonas syringae* suppresses host defense responses by activating JA signaling in a COI1-dependent manner (Katsir et al., 2008, (Zeng and He, 2010; Zhang et al., 2015;Zhou et al.,2015;Yang et al.,2019), these results showed that JA negatively regulates the *Pseudomonas syringae* resistance. However, in the present study, results showed that JA positively regulates the bacterial wilt resistance. In tomato, the JA-dependent signaling pathway is required for biocontrol agent-induced resistance against *R. solanacearum*. Jiang et al. (2019) showed that silicon treatment increases the contents of SA and JA and SA and JA-related genes to improve the bacterial wilt resistance of tomato. In future studies, the functions of JA in response of eggplant to *R. solanacearum* will be analyzed.

CONCLUSIONS

The integrated transcriptomic and metabolomic analysis generated a set of data to reveal the defense response of eggplant to bacterial wilt. Defense responses include the biosyntheses of flavone and flavonoids and phytohormones. The gene expression and metabolic networks identified in this study provide new insights into the mechanisms of induced defense response in eggplant. Our results will remarkably improve our knowledge of the bacterial wilt resistance mechanism of eggplant and provide clues for the development of resistant eggplant varieties.

Funding

This research was supported by National Natural Science Foundation of China (No. 31872117)，Central Public-interest Scientific Institution Basal Research Fund (No. 1630062022003), Central Public-interest Scientific Institution Basal Research Program for

Scientific Research Innovation Team (No. 1630062017014), and National Natural Science Foundation of Hainan Province (No. 321RC632)

Competing Interests

The authors declare there are no competing interests.

Author Contributions

Xiao XO designed the experiment and composed the manuscript. Lin WQ analyzed the DEG data and revised the manuscript. Feng EY investigated and analyzed the disease index. Ou XC analyzed the metabolome data and revised the manuscript.

Figure captions

Figure 1 Analysis of eggplant bacterial wilt resistance. Figure 1 Analysis of eggplant bacterial wilt resistance . A, Disease index of R and S. B, Phenotype of wilt after inoculation with *R. solanacearum* at 10 days. C, EGFP fluorescence results at stem. D, EGFP fluorescence results at root. The red arrow indicates the EGFP fluorescence.

Figure 2 Differential gene expression of eggplant response to bacterial wilt. A, Principal component analysis (score plot) of all transcripts (RPKM values) detected in root. Data points represent different samples. B, Clustering analysis and heat map of expression measures of DEGs detected in each of the experimental conditions. C, Numbers of upregulated and downregulated genes after inoculation with bacterial wilt over time.

Figure 3. Venn diagram showing overlap of upregulated and downregulated genes of eggplant response to bacterial wilt.

Figure 4 Clustering and classification of DEGs in eggplant response bacterial wilt.

Figure 5 Differential metabolites of eggplant in response to bacterial wilt. A, Principal component analysis of all metabolites detected in root. Data points represent different samples. B, Clustering analysis and heat map of expression measures of DEGs detected in each of the experimental conditions. C, Numbers of upregulated and downregulated metabolites after inoculation of R. *solanacearum*.

Figure 6 Venn diagram showing overlap of upregulated and downregulated metabolites of eggplant response to bacterial wilt.

Figure 7 Clustering and classification of differential metabolites in eggplant response to bacterial wilt.

Figure 8 Gene–metabolite correlation network representing the genes and metabolites involved in the bacterial wilt resistance of eggplant. A, Ko00592 network of R-0h vs. R-24h group. B, Ko04075 network of R-0h vs R-24h group. C, Ko04075 network of R-0h vs. R-48h group. Red and green dots indicate genes and metabolites, respectively.

Figure 9 Heat maps of genes involved in the JA biosynthesis and signaling cascade after inoculation with *R. solanacearum*.

Supplementary Materials:

Figure S1 KEGG classification of DEGs in eggplant after inoculation with *R. solanacearum.*

Figure S2 KOG classification of eggplant after inoculation with *R. solanacearum.*

Figure S3 KEGG classification of differentially expressed metabolites in eggplant after inoculation with *R. solanacearum*.

Figure S4 KEGG enrichment P-value histogram of DEGs and differentially expressed metabolites.

Figure S5 KEGG pathway of alpha-Linolenic acid metabolism and plant hormone signal transduction pathway during eggplant response to *R. solanacearum.*

Table S1 DEGs of eggplant after inoculation with *R. solanacearum* in R-0h_vs_R-24h.

Table S2 DEGs of eggplant after inoculation with *R. solanacearum* in R-0h_vs_R-48h.

Table S3 DEGs of eggplant after inoculation with *R. solanacearum* in R-24h_vs_R-48h.

Table S4 666 metabolites detected in eggplant after inoculation with *R. solanacearum.*

Table S5 Differential metabolites of eggplant after inoculation with *R. solanacearum* in R-0h_vs_R-24h.

Table S6 Differential metabolites of eggplant after inoculation with *R. solanacearum* in R-0h_vs_R-48h.

Table S7 Differential metabolites of eggplant after inoculation with *R. solanacearum* in R-24h_vs_R-48h.

Table S8 69 genes involved in alpha-Linolenic acid metabolism and plant hormone signal transduction pathway during eggplant response to *R. solanacearum*.

REFERENCES

Abebe AM, Choi J, Kim Y, Oh CS, Yeam I, Nou IS, and Lee JM. 2020. Development of diagnostic molecular markers for marker-assisted breeding against bacterial wilt in tomato. *Breed Sci* 70:462-473.

Ayana G, and Fininsa C. 2017. Effect of Crop Rotation on Tomato Bacterial Wilt (*Ralstonia solanacearum*) and Survival of the Pathogen in the Rhizospheres and Roots of Different Crops in Ethiopia. *Int J Phytopathol* 5(3):81-88.

Barchi L, Pietrella M, Venturini L, Minio A, Toppino L, Acquadro A, Andolfo G, Aprea G, Avanzato C, Bassolino L, Comino C, Molin AD, Ferrarini A, Maor LC, Portis E, Reyes-Chin-Wo S, Rinaldi R, Sala T, Scaglione D, Sonawane P, Tononi P, Almekias-Siegl E, Zago E, Ercolano MR, Aharoni A, Delledonne M, Giuliano G, Lanteri S, and Rotino GL. 2019. A chromosome-anchored eggplant genome sequence reveals key events in Solanaceae evolution. *Sci Rep* 9:11769.

Barik S, Reddy AC, Ponnam N, Kumari M, C AG, Reddy D C L, Petikam S, and Gs S. 2020. Breeding for bacterial wilt resistance in eggplant (*Solanum melongena* L.): Progress and prospects. *Crop Protection* 137:105270.

Chen F, Ma R, and Chen XL. 2019. Advances of Metabolomics in Fungal Pathogen-Plant Interactions. *Metabolites* 9. DOI: 10.3390/metabo9080169

Chen N, Yu B, Dong R, Lei J, Chen C, and Cao B. 2018. RNA-Seq-derived identification of differential transcription in the eggplant (*Solanum melongena*) following inoculation with bacterial wilt. *Gene* 644:137-147.

Dai F, Luo G, Wang Z, Kuang Z, Li Z, Huang J, and Tang C. 2019. Possible involvement of flavonoids in response of mulberry (*Morus alba* L.) to infection with Ralstonia solanacearum (Smith 1896) Yabuuchi et al., 1996. *European Journal of Horticultural Science* 84:161-170.

Dong X. 1998. SA, JA, ethylene, and disease resistance in plants. *Current Opinion in Plant Biology* 1:316-323.

Feys BJ, and Parker JE. 2000. Interplay of signaling pathways in plant disease resistance. *Trends in Genetics* 16:449-455.

Gurbuz N, Uluisik S, Frary A, Frary A, and Doganlar S. 2018. Health benefits and bioactive compounds of eggplant. *Food Chem* 268:602-610.

Habe I, Miyatake K, Nunome T, Yamasaki M, and Hayashi T. 2019. QTL analysis of resistance to bacterial wilt caused by *Ralstonia solanacearum* in potato. *Breed Sci* 69:592-600.

392 Ishihara T, Mitsuhara I, Takahashi H, and Nakaho K. 2012. Transcriptome analysis of quantitative resistance-
393 specific response upon *Ralstonia solanacearum* infection in tomato. *PLoS One* 7:e46763.
394 Jiang G, Wei Z, Xu J, Chen H, Zhang Y, She X, Macho AP, Ding W, and Liao B. 2017. Bacterial Wilt in China:
395 History, Current Status, and Future Perspectives. *Front Plant Sci* 8:1549.
396 Jiang N, Fan X, Lin W, Wang G, and Cai K. 2019. Transcriptome Analysis Reveals New Insights into the Bacterial
397 Wilt Resistance Mechanism Mediated by Silicon in Tomato. *Int J Mol Sci* 20.
398 Kim B, Hwang IS, Lee HJ, Lee JM, Seo E, Choi D, and Oh CS. 2018. Identification of a molecular marker tightly
399 linked to bacterial wilt resistance in tomato by genome-wide SNP analysis. *Theor Appl Genet* 131:1017-
400 1030.
401 Kumar L, Futschik ME.2007. Mfuzz: a software package for soft clustering of microarray data. *Bioinformation*.
402 20;2(1):5-7. doi: 10.6026/97320630002005
403 Li P, Ruan Z, Fei Z, Yan J, and Tang G. 2021a. Integrated Transcriptome and Metabolome Analysis Revealed That
404 Flavonoid Biosynthesis May Dominate the Resistance of Zanthoxylum bungeanum against Stem Canker. *J*
405 *Agric Food Chem* 69:6360-6378.
406 Li S, Deng B, Tian S, Guo M, Liu H, and Zhao X. 2021b. Metabolic and transcriptomic analyses reveal different
407 metabolite biosynthesis profiles between leaf buds and mature leaves in Ziziphus jujuba mill. *Food Chem*
408 347:129005.
409 Li Y, Wang L, Sun G, Li X, Chen Z, Feng J, and Yang Y. 2021c. Digital gene expression analysis of the response to
410 *Ralstonia solanacearum* between resistant and susceptible tobacco varieties. *Sci Rep* 11:3887.
411 Love MI, Huber W, Anders S. 2014. Moderated estimation of fold change and dispersion for RNA-seq data with
412 DESeq2. Genome Biology 15:550
413 DOI 10.1186/s13059-014-0550-8.
414 Luo H, Pandey MK, Khan AW, Wu B, Guo J, Ren X, Zhou X, Chen Y, Chen W, Huang L, Liu N, Lei Y, Liao B,
415 Varshney RK, and Jiang H. 2019. Next-generation sequencing identified genomic region and diagnostic
416 markers for resistance to bacterial wilt on chromosome B02 in peanut (*Arachis hypogaea* L.). *Plant*
417 *Biotechnol J* 17:2356-2369.
418 Manickam R, Chen JR, Sotelo-Cardona P, Kenyon L, and Srinivasan R. 2021. Evaluation of Different Bacterial Wilt

Resistant Eggplant Rootstocks for Grafting Tomato. *Plants* (Basel) 10(1):75

Na C, Shuanghua W, Jinglong F, Bihao C, Jianjun L, Changming C, and Jin J. 2016. Overexpression of the Eggplant (*Solanum melongena*) NAC Family Transcription Factor SmNAC Suppresses Resistance to Bacterial Wilt. *Sci Rep* 6:31568.

Salgon S, Jourda C, Sauvage C, Daunay MC, Reynaud B, Wicker E, and Dintinger J. 2017. Eggplant Resistance to the *Ralstonia solanacearum* Species Complex Involves Both Broad-Spectrum and Strain-Specific Quantitative Trait Loci. *Front Plant Sci* 8:828.

Salgon S, Raynal M, Lebon S, Baptiste JM, Daunay MC, Dintinger J, and Jourda C. 2018. Genotyping by Sequencing Highlights a Polygenic Resistance to Ralstonia pseudosolanacearum in Eggplant (*Solanum melongena* L.). *Int J Mol Sci* 19.

Schauer N, and Fernie AR. 2006. Plant metabolomics: towards biological function and mechanism. *Trends Plant Sci* 11:508-516.

Shulaev V, Cortes D, Miller G, and Mittler R. 2008. Metabolomics for plant stress response. *Physiol Plant* 132:199-208.

Su P, Zhao L, Li W Zhao J, Yan J, Ma X, Li A, Wang H, and Kong L.2021. Integrated metabolo-transcriptomics and functional characterization reveals that the wheat auxin receptor TIR1 negatively regulates defense against *Fusarium graminearum*. *J Integr Plant Biol* 63(2): 340-352.

Wang L, Zhou X, Ren X, Huang L, Luo H, Chen Y, Chen W, Liu N, Liao B, Lei Y, Yan L, Shen J, and Jiang H. 2018. A Major and Stable QTL for Bacterial Wilt Resistance on Chromosome B02 Identified Using a High-Density SNP-Based Genetic Linkage Map in Cultivated Peanut Yuanza 9102 Derived Population. *Front Genet* 9:652.

Wei Y, Zhang Y, Meng J, Wang Y, Zhong C, and Ma H. 2021. Transcriptome and metabolome profiling in naturally infested Casuarina equisetifolia clones by *Ralstonia solanacearum*. *Genomics* 113:1906-1918.

Xi-ou X, Wenqiu L, Zuo C, Chunxiang Z, Hui J, and Huafen Z. 2021. Wide-host Vector pBBR1MCS2-Tac-EGFP Suitable for the Labeling of *Ralstonia solanacearum*. *Chinese Journal of Tropical Crops* 42:1700-1705.

Yang J, Duan G, Li C, Liu L, Han G, Zhang Y, and Wang C .2019. The Crosstalks Between Jasmonic Acid and Other Plant Hormone Signaling Highlight the Involvement of Jasmonic Acid as a Core Component in Plant

Response to Biotic and Abiotic Stresses. *Front Plant Sci* 10:1349 doi: 103389/fpls201901349

Yang X, Zhang Y, Cheng Y, and Chen X. 2019. Transcriptome analysis reveals multiple signal network contributing to the Verticillium wilt resistance in eggplant. *Scientia Horticulturae* 256:108576.

Yuan H, Zeng X, Yang Q, Xu Q, Wang Y, Jabu D, Sang Z, and Tashi N. 2018. Gene coexpression network analysis combined with metabonomics reveals the resistance responses to powdery mildew in Tibetan hulless barley. *Sci Rep* 8:14928.

Yuya U, Shiduku T, Daisuke T, Hodaka S, Kazuya A, and KenjiG. 2016. Overexpression of OsMYC2 Results in the Up-Regulation of Early JA-Rresponsive Genes and Bacterial Blight Resistance in Rice. *Plant Cell Physiol* 59(9):1814–1827, https://doiorg/101093/pcp/pcw101

Yuliar, Nion YA, and Toyota K. 2015. Recent trends in control methods for bacterial wilt diseases caused by *Ralstonia solanacearum*. *Microbes Environ* 30:1-11.

Zaynab M, Fatima M, Abbas S, Sharif Y, Umair M, Zafar MH, and Bahadar K. 2018. Role of secondary metabolites in plant defense against pathogens. *Microb Pathog* 124:198-202.

Zeiss DR, Mhlongo MI, Tugizimana F, Steenkamp PA, and Dubery IA. 2018. Comparative Metabolic Phenotyping of Tomato (*Solanum lycopersicum*) for the Identification of Metabolic Signatures in Cultivars Differing in Resistance to *Ralstonia solanacearum*. *Int J Mol Sci* 19.

Zeiss DR, Mhlongo MI, Tugizimana F, Steenkamp PA, and Dubery IA. 2019. Metabolomic Profiling of the Host Response of Tomato (*Solanum lycopersicum*) Following Infection by *Ralstonia solanacearum*. *Int J Mol Sci* 20 20(16):3945..

Zeng W, and He SY .2010. A prominent role of the flagellin receptor FLAGELLIN-SENSING2 in mediating stomatal response to *Pseudomonas syringae* pv tomato DC3000 in Arabidopsis. Plant Physiol 153 (3), 1188–1198 doi: 102307/25704949

Zhang S, and Klessig DF. 2001. MAPK cascades in plant defense signaling. *Trends in Plant Science* 6:520-527.

Zhang L, Yao J, Withers J, Xin X-F, Banerjee R, Fariduddin Q .2015.Host target modification as a strategy to counter pathogen hijacking of the jasmonate hormone receptor. Proc Natl Acad Sci U S A 112, 14354–14359 doi: 101073/pnas1510745112

Zhao C, Wang H, Lu Y, Hu J, Qu L, Li Z, Wang D, He Y, Valls M, Coll NS, Chen Q, and Lu H. 2019. Deep

Sequencing Reveals Early Reprogramming of Arabidopsis Root Transcriptomes Upon *Ralstonia solanacearum* Infection. *Mol Plant Microbe Interact* 32:813-827.

Zuluaga AP, Solé M, Lu H, Góngora-Castillo E, Vaillancourt B, Coll N, Buell CR, and Valls M. 2015. Transcriptome responses to *Ralstonia solanacearum* infection in the roots of the wild potato *Solanum commersonii*. *BMC Genomics* 16:246.

480

481

482

483

484

Figure 1

Figure 1 Analysis of eggplant bacterial wilt resistance.

Figure 1 Analysis of eggplant bacterial wilt resistance . A, Disease index of R and S. B, Phenotype of wilt after inoculation with *R. solanacearum* at 10 days. C, EGFP fluorescence results at stem. D, EGFP fluorescence results at root. The red arrow indicates the EGFP fluorescence.

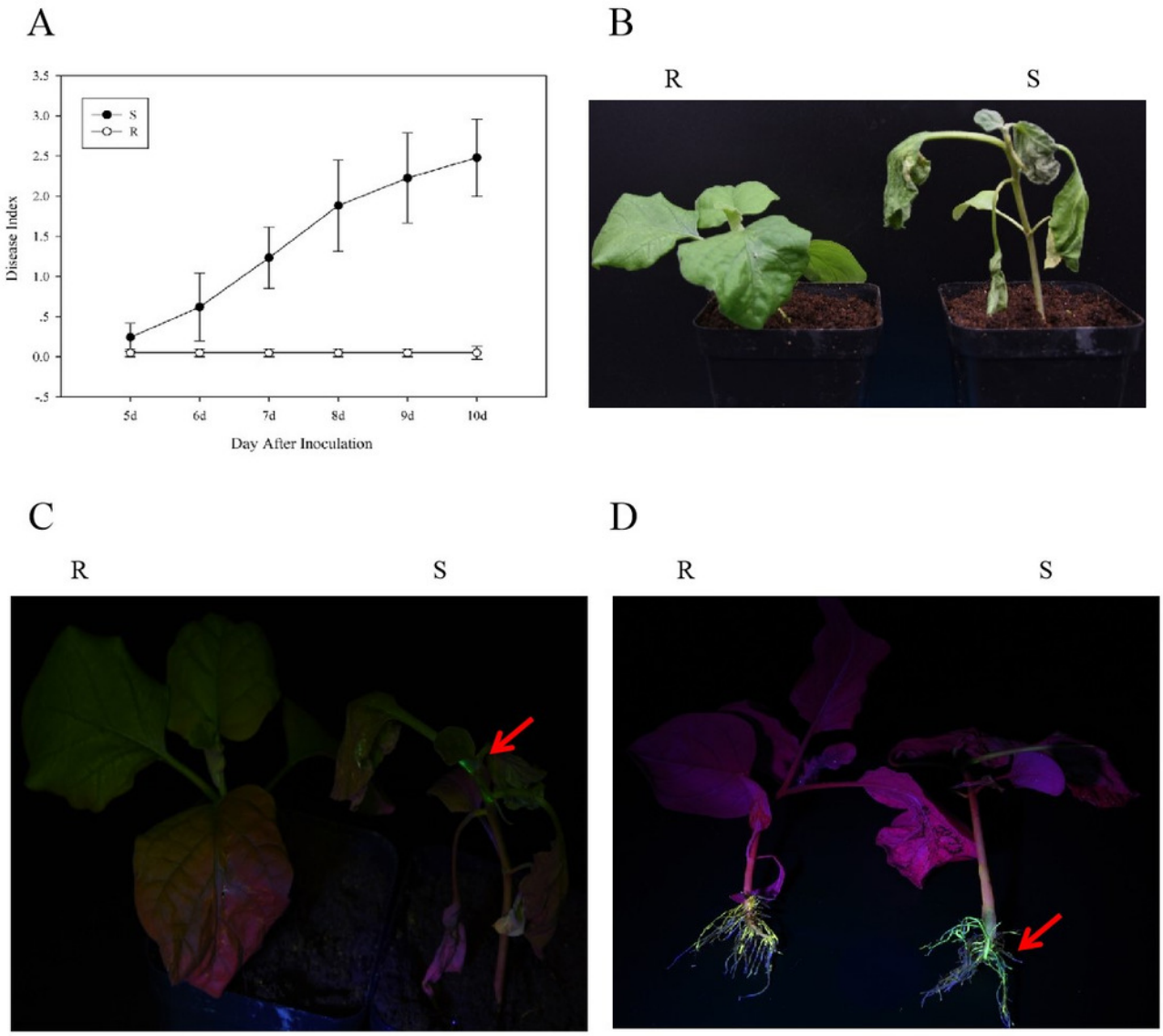

Figure 2

Figure 2 Differential gene expression of eggplant response to bacterial wilt

A, Principal component analysis (score plot) of all transcripts (RPKM values) detected in root. Data points represent different samples. B, Clustering analysis and heat map of expression measures of DEGs detected in each of the experimental conditions. C, Numbers of upregulated and downregulated genes after inoculation with bacterial wilt over time.

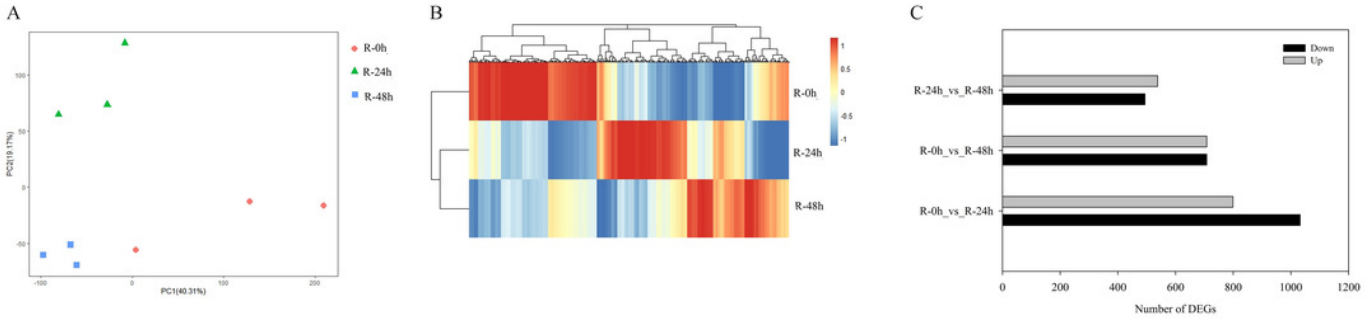

Figure 3

Figure 3. Venn diagram showing overlap of upregulated and downregulated genes of eggplant response to bacterial wilt.

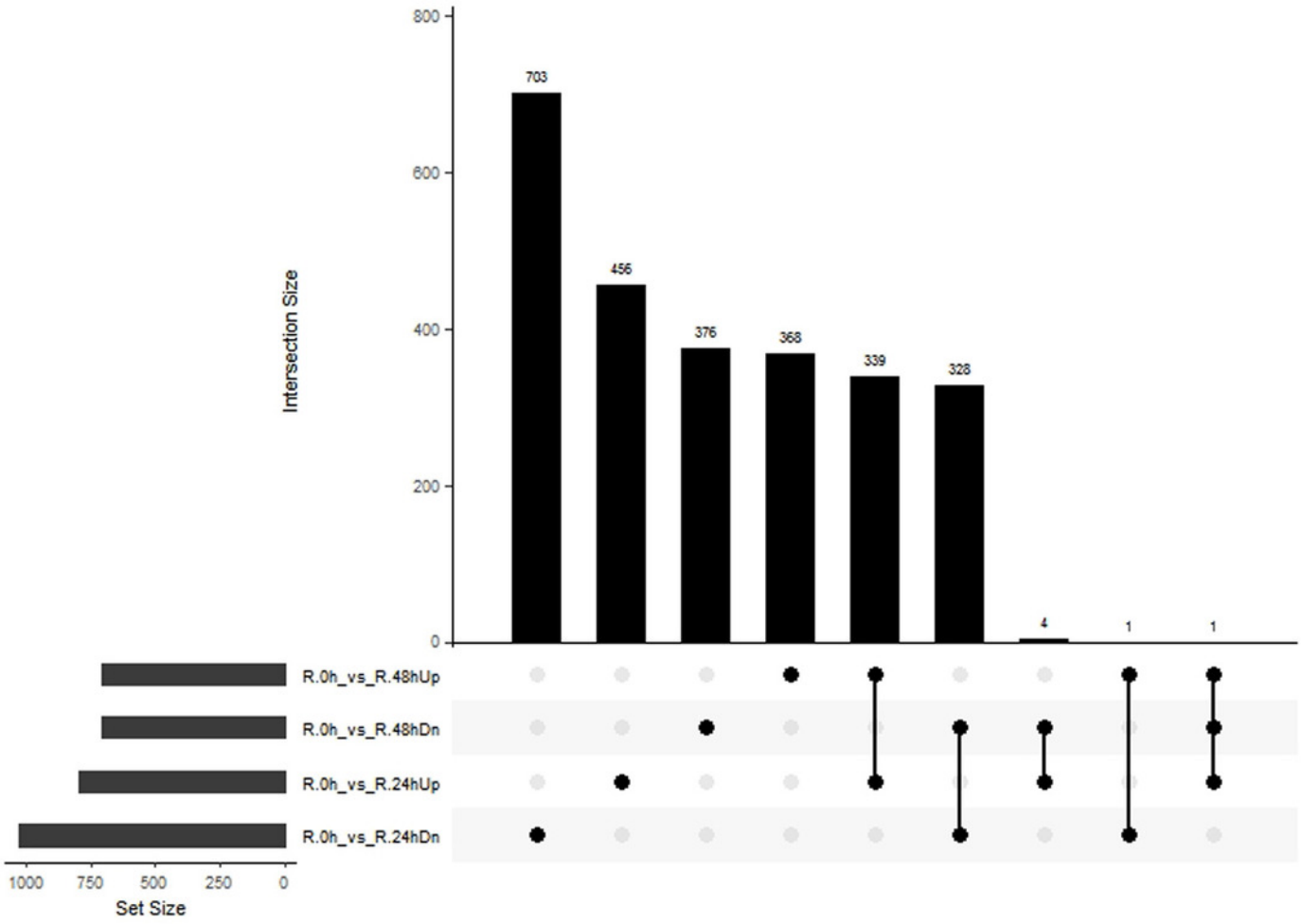

Figure 4

Figure 4 Clustering and classification of DEGs in eggplant response bacterial wilt.

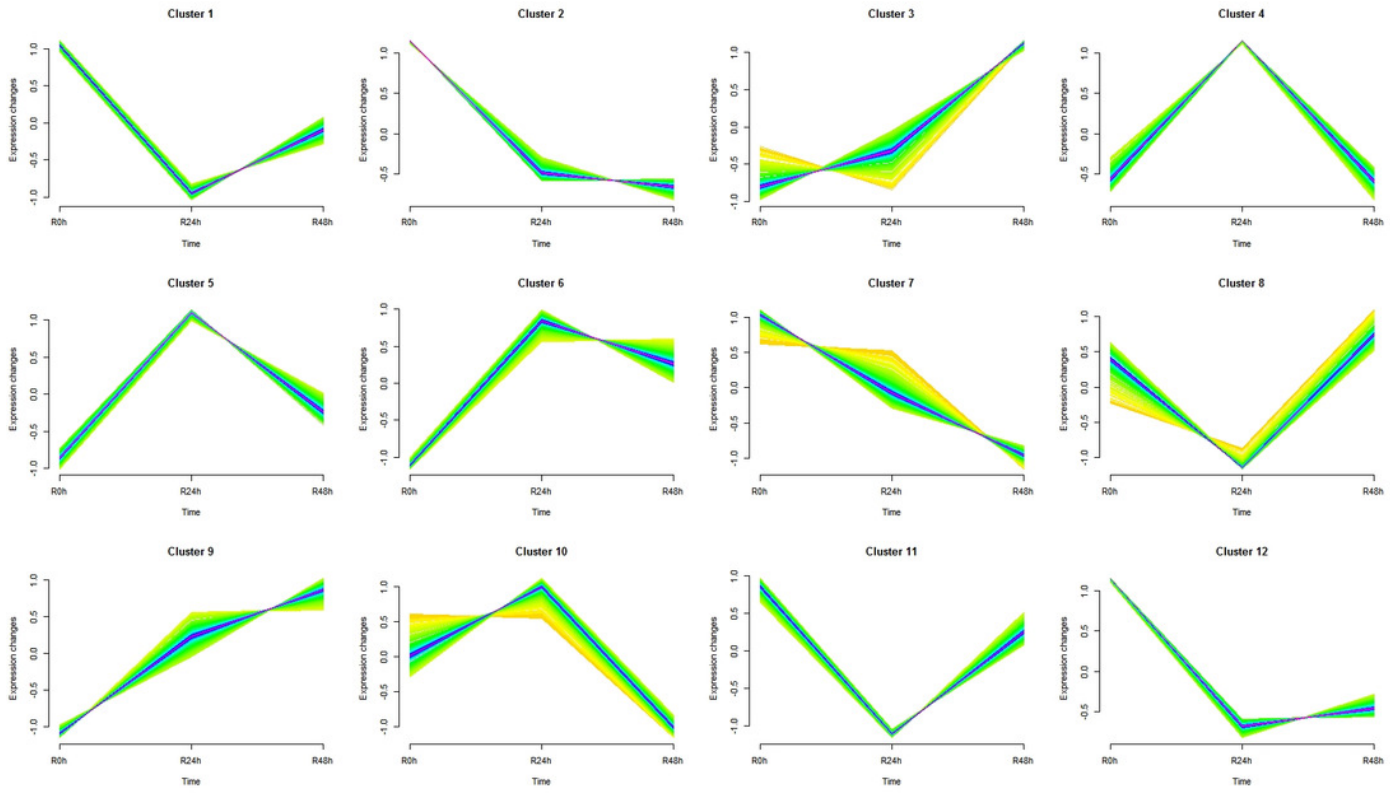

Figure 5

Figure 5 Differential metabolites of eggplant in response to bacterial wilt

A, Principal component analysis of all metabolites detected in root. Data points represent different samples. B, Clustering analysis and heat map of expression measures of DEGs detected in each of the experimental conditions. C, Numbers of upregulated and downregulated metabolites after inoculation of *R. solanacearum.*

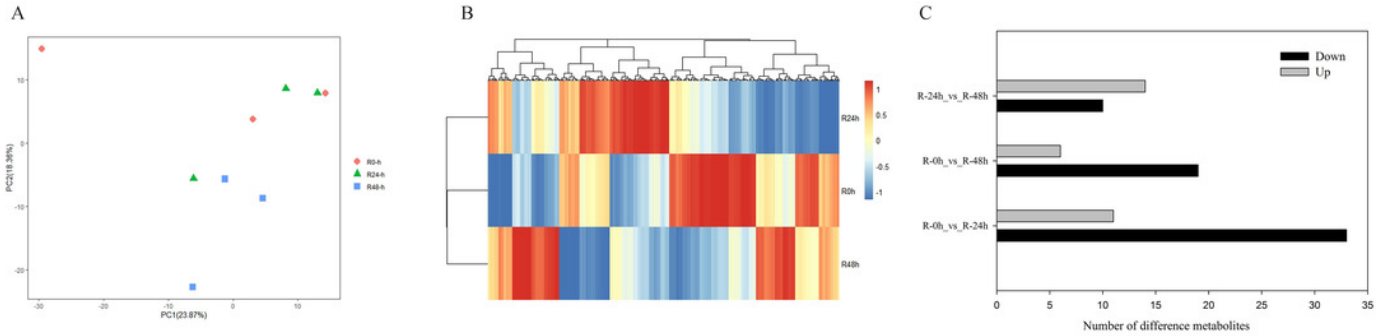

Figure 6

Figure 6 Venn diagram showing overlap of upregulated and downregulated metabolites of eggplant response to bacterial wilt.

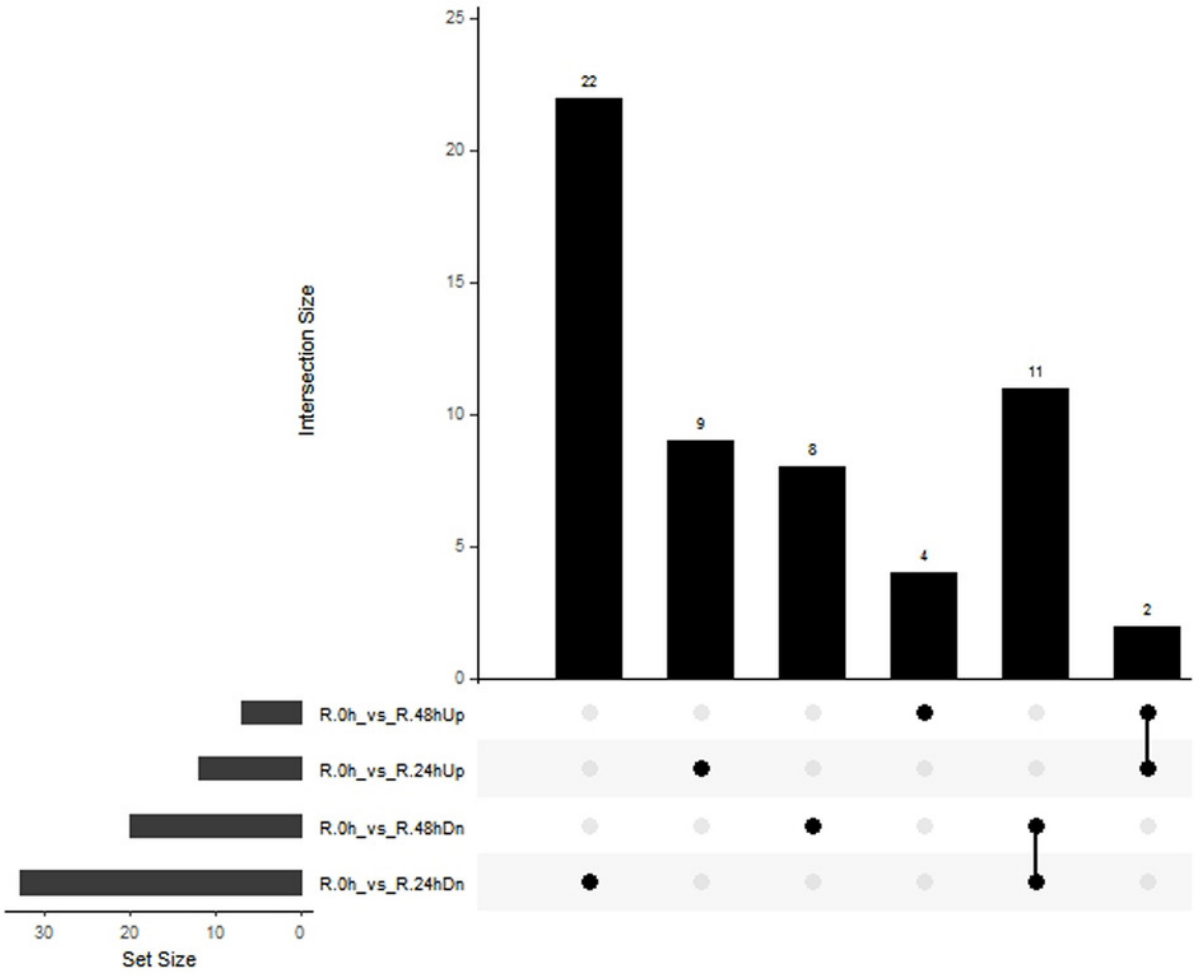

Figure 7

Figure 7 Clustering and classification of differential metabolites in eggplant response to bacterial wilt.

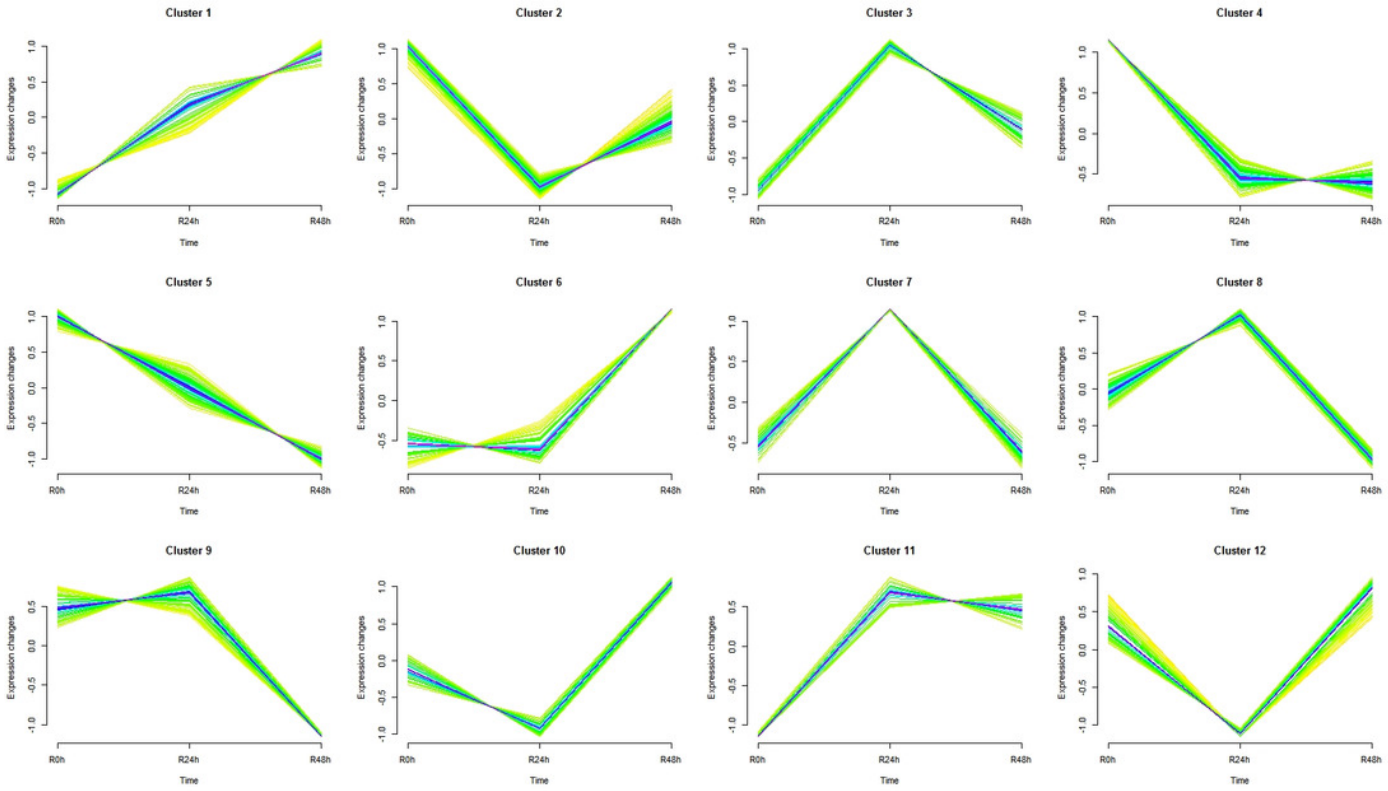

Figure 8

Figure 8 Gene–metabolite correlation network representing the genes and metabolites involved in the bacterial wilt resistance of eggplant.

Figure 8 Gene–metabolite correlation network representing the genes and metabolites involved in the bacterial wilt resistance of eggplant. A, Ko00592 network of R-0h vs. R-24h group. B, Ko04075 network of R-0h vs R-24h group. C, Ko04075 network of R-0h vs. R-48h group. Red and green dots indicate genes and metabolites, respectively.

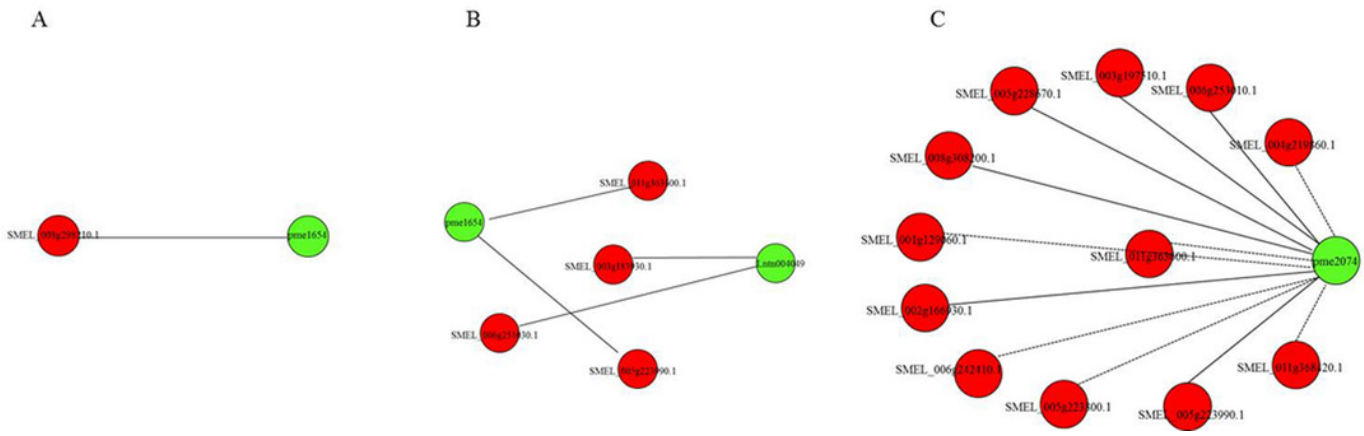

Figure 9

Figure 9 Heat maps of genes involved in the JA biosynthesis and signaling cascade after inoculation with *R. solanacearum.*

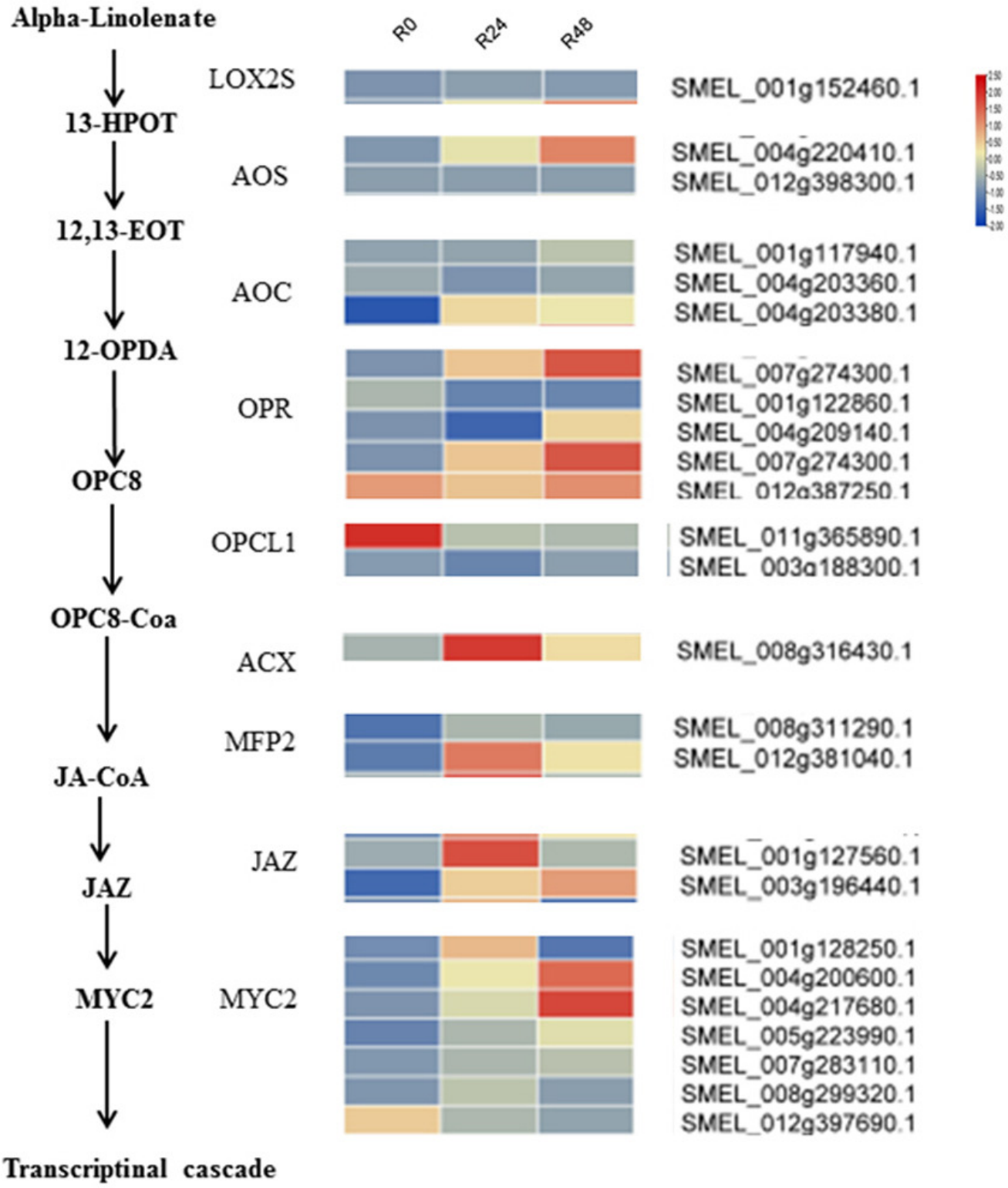
Alpha-Linolenate
13-HPOT
12,13-EOT
12-OPDA
OPC8
OPC8-Coa
JA-CoA
JAZ
MYC2
Transcriptinal cascade
LOX2S
AOS
AOC
OPR
OPCL1
ACX
MFP2
JAZ
MYC2
R0
R24
R48
SMEL_001g152460.1
SMEL_004g220410.1
SMEL_012g398300.1
SMEL_001g117940.1
SMEL_004g203360.1
SMEL_004g203380.1
SMEL_007g274300.1
SMEL_001g122860.1
SMEL_004g209140.1
SMEL_007g274300.1
SMEL_011g365890.1
SMEL_008g316430.1
SMEL_008g311290.1
SMEL_012g381040.1
SMEL_001g127560.1
SMEL_003g196440.1
SMEL_001g128250.1
SMEL_004g200600.1
SMEL_004g217680.1
SMEL_005g223990.1
SMEL_007g283110.1
SMEL_008g299320.1
SMEL_012g397690.1

Table 1(on next page)

Tabel 1 Summary of RNA-Seq and mapping results

1 Tabel 1 Summary of RNA-Seq and mapping results

Sample	Clean Reads	Reads mapped	Unique mapped
R0h-1	44682626	37833014(84.67%)	35475538(79.39%)
R0h-2	49200972	41973818(85.31%)	39310684(79.90%)
R0h-3	43577276	37139673(85.23%)	34776165(79.80%)
R24h-1	42181106	35684002(84.60%)	33436786(79.27%)
R24h-2	47172092	39987170(84.77%)	37498014(79.49%)
R24h-3	41443394	35095278(84.68%)	32848381(79.26%)
R48h-1	39695734	33712594(84.93%)	31702472(79.86%)
R48h-2	42944098	36503682(85.00%)	34249420(79.75%)
R48h-3	40078694	34034257(84.92%)	31930569(79.67%)

2